Novel Carbazole Dendrimers Having a Metal Coordination Site as a Unique Hole-Transport Material

*Atsushi Kimoto, Jun-Sang Cho, Masayoshi Higuchi, Kimihisa Yamamoto**

Kanagawa Academy of Science & Technology (KAST), and Department of Chemistry, Faculty of Science & Technology, Keio University, Yokohama, 223-8522 (Japan)
E-mail: yamamoto@chem.keio.ac.jp

Summary: We have synthesized novel carbazole dendrimers via the cyclotrimerization of aminophenylketones in the presence of titanium tetrachloride. These dendrimers have the ability to assemble metal ions such as Sn^{2+} and Eu^{3+} with no significant difference in their generation, suggesting the dendrimer with an interior with a small density up to the third generation. We show the dendrimers with higher generations have the higher HOMO values. The most electron rich molecule, the G3 dendrimer, has the highest HOMO value of −5.2 eV. However, for the HOMO energy levels of the carbazole dendrimer complex with $Eu(OTf)_3$, the energy levels of the carbazoles did not change based on almost the same redox potentials as those of the dendrimers, themselves. Using the carbazole dendrimers and their europium complex, a homogeneous film was produced, which enhanced the performance of the electroluminescence device in comparison with only the dendrimer as the hole-transporting layer. This approach was managed by a solution process, i.e., the spin-coating method, without using the coevaporation technique based on the large equilibrium constants of the coordination of metal ions on the imine sites ($K = 10^5\ M^{-1}$).

Keywords: carbazole; dendrimers; electroluminescence; hole transport; metal-polymer complexes

Introduction

Discrete triphenylamine arrays based on linear,[1] cyclic,[2] and dendritic[3] systems with a conjugated backbone display attractive magnetic and electronic properties. Also, acting as hole-transport materials in various electro-optical applications, for example, organic light-emitting diodes (OLEDs)[4] and photocells,[5] branched and dendritic structures exhibit a better amorphous property and high solubility due to the geometry of these molecules without close packing. Above all, dendrimers consisting of a core, dendrons, and peripheral units can be easily designed

 DOI: 10.1002/masy.200450504

by modular synthesis, however, hyper-branched polymers cannot. We should note that dendrimers, especially rigid ones, can possibly be regularly assembled by packing on a plate without deformation of the molecule[6] and are expected to expand the field of nanomaterials.[7]

Organic materials for various electro-optical applications generally consist of rigid π-conjugated structures with a narrow HOMO-LUMO gap. Above all, a number of dendrimers have been used in OLEDs[8] designed by their characteristic synthetic procedure, the convergent method. The advantages of adopting monodisperse and well-defined dendrimers as active components in OLEDs are that they can be easily prepared in high purity and have a better amorphous property and high solubility due to their geometry without close packing, resulting in the easier fabrication of thin films by the spin-coating method, a promising approach for large area display applications as well as polymeric components.

Efforts have been ongoing to develop a novel hole-transport polymer for advanced electronic devices. This is a key material for improving the turn-on voltage, luminescence intensity, operation lifetime, full color display capability, durability, reasonable power efficiency, and so on. Generally, such high-performance devices are obtained by developing sequential HOMO/LUMO energy gradients in the device by introducing the multi-layered structure fabricated by repeatedly making thin films. For example, introducing another layer on the ITO electrode, with a HOMO energy level between that of the hole-transporting layer and of the electrode, that is a hole-injecting layer, lowers the energy barrier for hole injection. This approach involves placing the injecting layer between the ITO and the transport layers, such as copper phtharocyanine (CuPc),[9] and 4, 4', 4''-tris(3-methylphenylphenylamino)triphenylamine (*m*-MTDATA),[8] which results in an enhanced EL efficiency. Another approach to develop the characteristics of the OLEDs has recently been raised by the insertion of thick doped materials such as doped triarylamine,[10] polyvinylcarbazole,[11] polythiophene,[12] and polyaniline,[13] resulting in the enhancement of a carrier injection and transport with a lower driving voltage. However, these two approaches require highly-layered structures, because of their molecular structures and syntheses, and the indefinite functional separation of the buffer and hole transport in one component. Moreover, the use of polymeric materials is restricted by the fabrication of such very complex structures because of the erosion of the fabricated film in advance followed by the method of making thin films, i.e., the spin coating method.

Here, we report the design of novel carbazole dendrimers having a phenylazomethine core as the metal coordination site. Also, the complexation with metal ions changes the properties of the dendrimer. Only complexation with metal ions results in a higher EL efficiency.

Results and Discussion

Synthesis

The G1, G2, and G3 carbazole dendrimers[14] were synthesized via the cyclotrimerization of the corresponding monomers in the presence of titanium (IV) tetrachloride (0.75 equiv.) and 1,4-diazabicyclo-[2.2.2]octane (DABCO) (1.5 equiv.) in 30, 56, and 95% yields, respectively (Scheme 1). The aminophenylketone monomers were prepared by a previously described method.[16] As a conventional synthetic technique to prepare the dendrimers, the convergent method results in a lower conversion yield by increasing the generation due to their steric hindrance of the bulky dendrons with a small core.[17] We developed a useful synthetic method for preparative dendrimer formation in which the core is generated from a dendritic precursor by a cyclization reaction.[18] Generally, the condensation of the *AB* type monomer only gives the corresponding linear polymer. Indeed, we have already reported that aminophenylketones such as 4-aminoacetophenone produce only the corresponding linear polymer, however, the reaction of the 4-aminobenzophenone derivatives provides the formation of cyclic phenylazomethines in high yield due to the steric hindrance of the bulky α-phenyl ring in the monomer.[19] Thus, this synthetic procedure to prepare dendrimers, especially with a higher generation, via the cyclization reaction were found to be an extremely effective method. These dendrimers were characterized by ^{1}H and ^{13}C NMR spectroscopies, and matrix-assisted laser desorption/ionization time-of-flight mass spectroscopy (MALDI-TOF-MS).

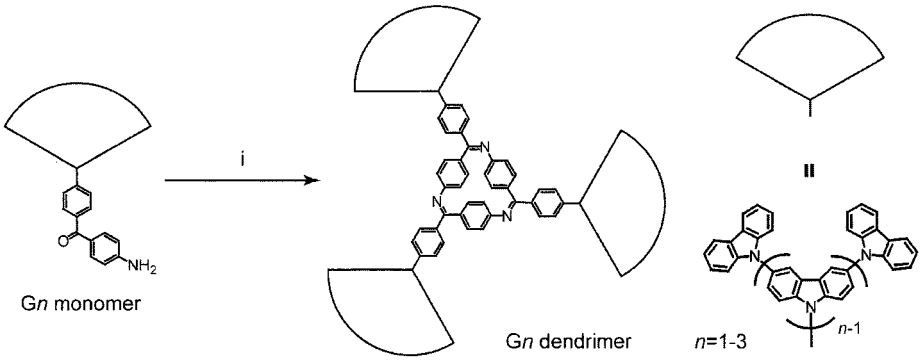

Scheme 1. Synthesis of the carbazole dendrimers[a]

[a] Reagents and conditions: (i) $TiCl_4$, DABCO, PhCl.

Optical Properties

The UV-vis spectra of the dendrimers show absorption bands at 300-425 nm (λ_{max}; 343 nm) attributed to the π-π^* transition of the cyclic phenylazomethine unit at the core and at 225-350 nm (λ_{max}; 294 nm) of the dendritic polycarbazole moiety. No significant red shifts in the absorption were observed (Table 1). This means that the degree of π delocalization is limited.[27] The absorption attributed to the carbazole unit proportionally intensifies as the number of carbazole units with the growth of their generation number, even though the absorption attributed to their core unit does not change. This localization is caused by the loss of coplanarity of the aromatic systems due to the twists in the polycarbazole dendrons at the 3 and 6 positions. The MM2 calculation also supported the fact that they are twisted by 36 degrees between the carbazole units. These dendrimers are expected to approach the sphere-like structure with higher generations. The photoluminescence spectra showed luminescence from the carbazole moieties that were quenched by the Förster type energy transfer to the imine unit.

Metal-Collecting Properties

The addition of $SnCl_2$ to a dichloromethane/acetonitrile solution of the dendrimers resulted in a complexation with a spectral change, similar to that for the previously reported dendrimers.[20] During the addition of $SnCl_2$, the solution color of the G3 dendrimer changed from light to deeper yellow. We observed that the complexation was complete in 10 minutes by the spectral change after the addition of $SnCl_2$, that is, the complexation equilibrium is reached within at least several minutes.[21] Using UV-vis spectroscopy to profile the complexation, only one isosbestic point was observed, indicating that the complexation randomly proceeds. Therefore, this observation suggests that the complexation behavior seen with the dendrimers does not reflect changes in the basicity of the imine sites induced by complexation at neighboring imine sites.

The absorption band around 400 nm attributed to the complex increases with a decrease in the absorption bands around 320 nm, attributed to the phenylazomethine unit. The spectra of the G3 dendrimer gradually changed, with an isosbestic point at 371 nm (Figure 1a). However, the spectral change did not finish upon the addition of $SnCl_2$ equivalent to the number of imine moieties (three imines) not likely observed in the complexation of other phenylazomethine dendrimers with $SnCl_2$.[20] This observation is based on the poor electron density on the imine site supported by the chemical shifts of the imine carbon of the dendrimers (about 169.5 ppm) compared to those of the phenylazomethines (about 168 ppm). The dendrimers were decomposed with an increase in the free $SnCl_2$, leading to another type of spectral change. Complexing with $Eu(OTf)_3$ (OTf; trifluoromethane sulfonate) instead of $SnCl_2$ as a Lewis acid, the absorption band around 400 nm attributed to the complex increases with a decrease in the absorption bands around 320 nm, also attributed to the phenylazomethine unit in the same way. The spectra of the G3 dendrimer gradually changed with an isosbestic point at 381 nm (Figure 1b). The spectral change finished upon the addition of 10 equivalents of $SnCl_2$ to the dendrimer without any decomposition. These results revealed that the complexation proceeds at random and the imine groups act as an excellent coordination site.

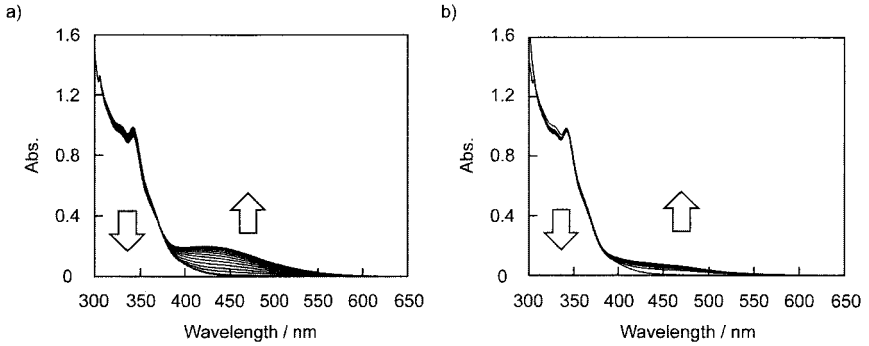

Figure 1. UV-vis spectra changes of the G3 dendrimer upon stepwise addition of equimolar a) $SnCl_2$ and b) $Eu(OTf)_3$ in CH_3CN/CH_2Cl_2 = 1/4.

Generally, a $SnCl_2$ molecule, which has one coordination site, is complexed with an imine site of phenylazomethine at the ratio of 1:1 (Figure 2a). On the other hand, for the complexation with $Eu(OTf)_3$, which has multi-coordination sites, the spectrum changed largely by addition of a small amount of $Eu(OTf)_3$ to the solution of the G3 dendrimer, resulting in a convex titration curve (Figure 2b). This phenomenon shows that a $Eu(OTf)_3$ molecule is complexed with several imine sites of the G3 dendrimer. The spectral change continued up to the addition of 10 equivalents of $Eu(OTf)_3$. This result shows that the complexation randomly occurs and the Eu salt is finally complexed with the imine site at the ratio of 1:1.

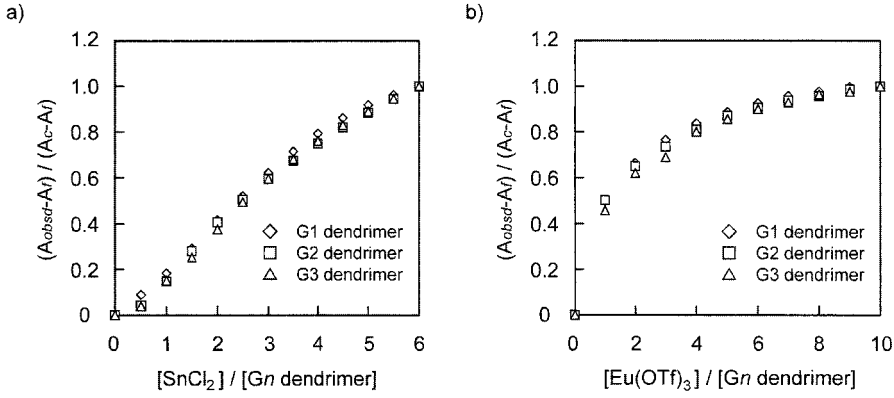

Figure 2. Titration curve changes of the G3 dendrimer upon stepwise addition of equimolar a) $SnCl_2$ and b) $Eu(OTf)_3$.

Comparing the generation number of the carbazole dendrimer, no significant difference in the complexation was observed, suggesting a dendrimer with an interior and an exterior with a small density up to the third generation. The equilibrium constants for the formation of 1:1 complexes with $SnCl_2$ (up to 6 equivalents to the dendrimer) and $Eu(OTf)_3$ on the imine sites were estimated to be $K = 10^5 (M^{-1})$. This estimation is based on the complexation behavior with the dendrimers indicating that the complexation randomly proceeds. We can transpose the cyclic phenylazomethine trimer unit to *three* monomeric phenylazomethine on the basis of the fact that the complexation at the neighboring imine site does not reflect changes in the basicity of the imine site.

Energy Levels of the Dendrimers

The electrochemical properties of the dendrimers (G1-G3) were studied by cyclic voltammetry. The HOMO values were determined from the first oxidation potential values with respect to ferrocene (-4.8 eV), as shown in Table 1. All the dendrimers displayed reversible oxidation waves attributed to the oxidation of triarylamines (the dendritic polycarbazole moiety) in the region between 0.2 V and 1.4 V *vs.* Fc/Fc^+. The oxidizability of the dendrimers decreased with the increasing generation number and decreasing electron richness, and therefore, the HOMO values gradually decreased from G3 (-5.2 eV) to G1 (-5.5 eV). Thus the most electron rich molecule, the G3 dendrimer, has the highest HOMO value of -5.2 eV and, accordingly, is expected to have the lowest barrier to hole injection from the ITO electrode (-4.8 eV) in OLEDs. By complexing with 1 equivalent of $Eu(OTf)_3$, redox waves with almost the same potential (-5.2 eV) as already observed in the oxidation wave of the dendron were seen. However, an additional stable redox wave attributed to the reduction of the azomethine-metal complex unit was not observed within the potential range.

Table 1. Physical data of the dendrimers

Compound	yield	λ_{max}	ε	$E_{1/2}^{ox}$	HOMO level
	%	nm	$mol^{-1}cm^{-1}$ a)	V vs.Fc/Fc^{+} b)	eV
G1 dendrimer	30	292	5 700	0.647, 0.919	-5.5
		343	7 200		
G2 dendrimer	56	294	6 300	0.521, 0.795	-5.3
		342	9 800		
G3 dendrimer	95	294	12 100	0.383, 0.677, 0.883 c)	-5.2
		343	13 200		
G3-Eu complex				0.414, 0.676, 0.869 c)	-5.2

a) Measured in THF. b) Measured in 1,2-dichloroethane. c) Taken from differential pulse voltammetry peaks.

Electroluminescence Properties Using the Dendrimers as HTL

A bright green emission was observed for all the cells when a positive dc voltage was applied to the ITO electrode. The electroluminescence spectrum was in accord with the photoluminescence spectrum of Alq. This indicates that the electroluminescence originates from the recombination of holes and electrons injected into Alq. Compared with the generations of the dendrimers, the maximum luminescence was 67.8 (G1), 497.3 (G2), and 786.4 (G3) cd/m^2 (Figure 3, Table 2). Also, the *I-V* characteristics are strongly dependent on their generation number. For example, the current density at 10 V increased from 5.11 mA/cm^2 (G1) to 53.6 mA/cm^2 (G3). This development is explained by the barriers ($\Delta\phi$) between the HOMO energy levels of the dendrimers and that of ITO, which are lowered in higher generations, resulting in enhanced hole injection and charge recombination. However, the G1 dendrimer, which has the HOMO energy level at -5.5 eV, close to that of TPD (N,N'-diphenyl-N,N'-di(*m*-tolyl)benzidine) (-5.5 eV), which is a commonly used hole transport compound, has shown a lower EL performance with a poor film-forming property based on the planarity in the smaller generation number. A simple molecular modeling has revealed that the G1 dendrimer has a planar structure, thus resulting in the crystalline formation of the film.

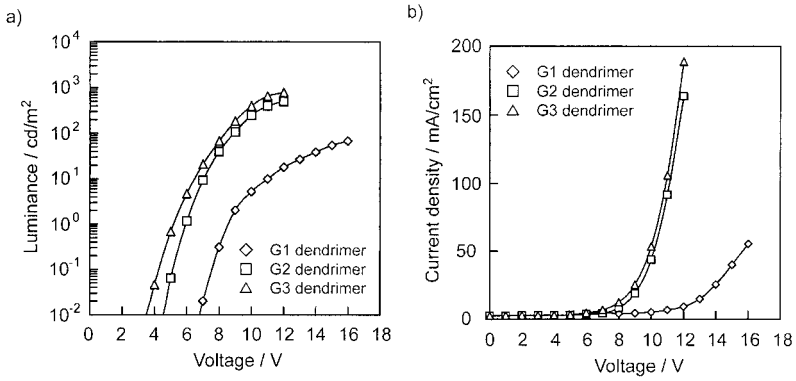

Figure 3. a) *L-V* and b) *I-V* characteristics of double-layer OLEDs with Al cathodes using the dendrimers as HTL.

For the two-layer OLEDs, the dendrimer complexes with the $Eu(OTf)_3$ films were then employed as the hole-transporting layer. We adopted $Eu(OTf)_3$ as a Lewis acid because of the stability of the dendrimer complex. From the spectral observation, the dendrimers were decomposed with an increase in the free $SnCl_2$. As shown in Figure 4 and Table 2, the low driving voltage and enhanced efficiency were followed by simply assembling of the metal ions. For the G3 dendrimer, the turn-on voltage was reduced from 4.3 V to 3.7 V and the maximum luminescence was enhanced from 786.4 cd/m^2 to 932 cd/m^2 by only complexing with $Eu(OTf)_3$. Also, the current performance of the G3-Eu complex was over three times greater (181.4 mA/cm^2) for the same forward driving voltage (10 V) compared to the uncomplexed device (53.6 mA/cm^2). The threshold voltages for obtaining a luminance of 100 cd/m^2 were 8.3 and 6.9 V for the cells, respectively. Considering the dendrimer complex as HTL, the characteristics of the devices are also strongly dependent on their generation number as seen in the device with the dendrimer itself as HTL. By inserting a thin CsF layer between the anode and electron transport layer, Alq, a significant improvement in the device has been obtained based on the enhancement of the electron injection and the performance of the device. The characteristics of the devices are also shown in Table 2. As measured, for the G3 dendrimer, the maximum luminescence was enhanced from 3 717 cd/m^2 to 6 718 cd/m^2 by applying a lower voltage, by

only complexing with $Eu(OTf)_3$ under the non-optimized conditions. These results indicate that the complexation with imine sites results in an increasing hole injection and/or transport efficiency from the electrode.

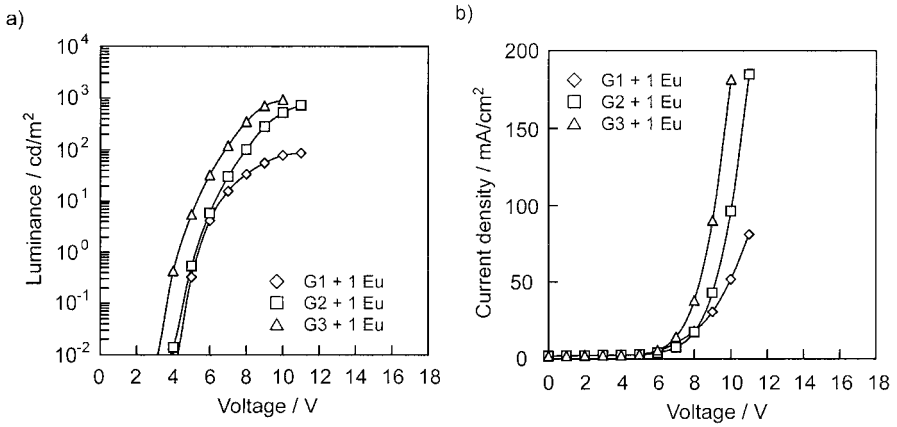

Figure 4. a) *L-V* and b) *I-V* characteristics of double-layer OLEDs with Al cathodes using the dendrimer complexes as HTL.

Table 2. Electroluminescence properties for the devices

HTLs	Turn-on voltage	Maximum luminance	Driving voltage	Current density	Power eff.
	V	cd/m^2	V [a]	mA/cm^2 [a]	lm/W [a]
G1 dendrimer	7.6	67.8			
G2 dendrimer	5.1	497.3	8.9	17.6	0.20
G3 dendrimer	4.3	786.4	8.3	15.6	0.24
G1+Eu complex	5.0	86.7			
G2+Eu complex	4.0	728.1	8.0	17.0	0.23
G3+Eu complex	3.7	932.0	6.9	12.2	0.37
G3 dendrimer [b]	5.0	3717	8.2	7.66	0.50
G3+Eu complex [b]	3.6	6178	5.1	5.86	1.05

a) Taken at 100 cd/m^2. b) Measured with the double-layer OLEDs having CsF(3 nm)/Al cathodes.

We described the controlled doping levels of the dendrimer and the OLED characteristics. Figure 5 shows the *I-V* characteristics of the ITO/G3 dendrimer + *n* Eu/Alq/Al devices (*n* = 0, 1, 2, 3, 3.6, 6) with the same configuration. The devices with the dendrimer complexes having up to the small amount of metal ions with a small excess showed a significant injection current density hardly depending on the amount of metal ions. On the other hand, with a large excess of metal ions (6 equivalents to the dendrimer), a lower current density was injected into the device, resulting in the lower efficiency. This is due to the increased free $Eu(OTf)_3$ and its high crystallinity in the polymer film.

For the HOMO energy levels of the carbazole dendrimer complex, the energy levels of the carbazoles did not change based on the same redox potentials when complexing. When considering the influence of doping on the turn-on voltage and the performance at a lower driving voltage, the reduction in the bulk resistance followed by the *p*-type doping facilitates efficient hole injection into the HTL. Also the reduction of space charge layers at the interface of the ITO and the dendrimer complex leads to efficient carrier injection due to tunneling. Recently, a controlled doping study has revealed that *p*-type doping leads to a higher conductivity for the doped triphenylamine layers and a high density of equilibrium charge carriers, which facilitates hole injection and transport, and producing the low operating voltage of the OLEDs.[22] The conductivity of the G3 dendrimer film with metal ions increases and is orders of magnitude higher than those of the dendrimer itself. The room temperature conductivity, measured by a two-probe method, of the G3 dendrimer complex with 1 equivalent of $Eu(OTf)_3$ was 1.2×10^{-4} S/cm. For comparison, the conductivity of the G3 dendrimer is below 10^{-6} S/cm in an environmentally controlled condition. By complexation, higher hole injection and transport were facilitated, thus resulting in a lower operating voltage of the OLEDs.[20,23]

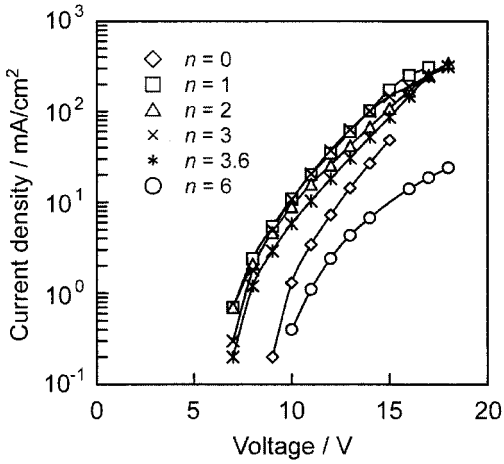

Figure 5. *I-V* characteristics of the ITO/G3 dendrimer + *n* Eu/Alq/Al devices (*n* = 0, 1, 2, 3, 3.6, 6).

Conclusion

A novel G3 carbazole dendrimer and its complex synthesized via the cyclotrimerization with a metal assembling property provide a homogeneous film which enhanced the performance of the electroluminescence device in comparison with only the G3 dendrimer as the hole-transporting layer. This is due to the enhancement of the conductivity by the *p*-type doping of the imine sites, resulting in better hole injection and transporting properties. This approach was managed by a solution process, i.e., spin-coating method, without using the coevaporation technique based on the large equilibrium constants of the coordination of metal ions on the imine sites ($K = 10^5 M^{-1}$).

Experimental Section

All chemicals were purchased from Aldrich, Tokyo Kasei Co., Ltd., and Kantoh Kagaku Co., Inc. (reagent grade) and used without further purification. The UV-vis spectra were obtained using a Shimadzu UV-2400PC spectrometer. The ^1H NMR and ^{13}C NMR spectra were measured on a JEOL 400 MHz FT-NMR (JMN 400). Cyclic voltammetry experiments were performed with a BAS-100 electrochemistry analyzer. All measurements were carried out at room temperature with a conventional three-electrode configuration consisting of a platinum working electrode, an

auxiliary platinum electrode, and a nonaqueous $Ag/AgNO_3$ reference electrode. The solvent in all experiments was 1,2-dichloroethane, and the supporting electrolyte was 0.1 M tetrabutylammonium hexafluorophosphate. The $E_{1/2}$ values were determined as $1/2(E_{pa}+E_{pc})$, where E_{pa} and E_{pc} are the anodic and cathodic peak potentials, respectively. All reported potentials are referenced to Fc^+/Fc external and are not corrected for the junction potential.

Conventional OLED devices having the ITO/dendrimer/Alq/Al structure were fabricated by spin-coating the dendrimer solutions in chlorobenzene on an ITO-coated glass anode. Alq (50 nm), and Al (100 nm) were successively vacuum deposited on top of the hole-transporting layer. The emitting area was 9 mm^2. The current-voltage characteristics were measured using an Advantest R6243 current/voltage unit. Luminance was measured with a Minolta LS-100 luminance meter in air at room temperature.

For the two-layer OLEDs, the dendrimer complexes with the $Eu(OTf)_3$ films, were then employed as the hole-transporting layer. To a solution of the dendrimer in chloroform was added a solution of $Eu(OTf)_3$ (1 equivalent *vs.* the dendrimers) in acetonitrile. The yellow solution changed to light orange based on the complexation, and evaporated to dryness to give the dendrimer complex. OLED devices having the ITO/dendrimer/Alq/CsF/Al structure were fabricated by spin-coating the dendrimer complex solutions in chlorobenzene on an ITO-coated glass anode. Alq (50 nm), CsF (2 nm) and Al (100 nm) were then successively vacuum deposited on top of the hole-transporting layer.

General Procedure for the Synthesis of the Gn Carbazole Dendrimers

To a mixture of the G*n* monomer (*n*=1-3) and DABCO in chlorobenzene was added dropwise $TiCl_4$. The addition funnel was then rinsed with chlorobenzene. The reaction mixture was heated in an oil bath at 125 °C for 22 h. The precipitate was removed by filtration. The filtrate was concentrated, and the residue was subjected to recycling SEC with THF as the eluent, where the fraction corresponding to the second major peak was collected and evaporated to dryness, to give the corresponding dendrimer

G1 Dendrimer. The previous procedure was followed using 0.272 g (0.187 mmol) of the G1 monomer, 0.246 g (2.19 mmol) of DABCO, and 0.104 g (0.547 mmol) of $TiCl_4$ in chlorobenzene (7.5 mL), to produce the G1 dendrimer as a yellow powder in 30% yield (0.077 g). ^1H NMR

(400 MHz, $CDCl_3$, TMS standard, 30 °C, ppm): δ 8.16 (d, 7.6 Hz, 6H), 8.15 (d, J=8.2 Hz, 6H), 7.69 (d, J=7.6 Hz, 6H), 7.52 (d, J=7.6 Hz, 6H), 7.44 (dd, J=7.4, 8.2 Hz, 6H), 7.32 (dd, J=7.6, 7.4 Hz, 6H), 6.95 (d, 7.6 Hz, 6H), 6.66 (d, J=7.6 Hz, 6H). ^{13}C NMR (100 MHz, $CDCl_3$, TMS standard, 30 °C, ppm): δ 170.23, 152.63, 140.35, 140.27, 136.62, 130.61, 128.10, 126.38, 126.00, 123.57, 120.30, 120.25, 119.73, 109.72. MALDI-TOF-MS: 1032.4 ($[M]^+$ calcd for $C_{75}H_{48}N_6$: 1032.4).

G2 Dendrimer. The previous procedure was followed using 0.520 g (0.750 mmol) of the G2 monomer, 0.253 g (2.25 mmol) of DABCO, and 0.107 g (0.563 mmol) of $TiCl_4$ in chlorobenzene (7.5 mL), to produce the G2 dendrimer as a yellow powder in 56% yield (0.283 g). ^1H NMR (400 MHz, $CDCl_3$, TMS standard, 30 °C, ppm): δ 8.30(s, 6H), 8.28(d, J=11.2 Hz, 6H), 8.17(d, J=7.2 Hz, 12H), 7.87(d, J=8.8 Hz, 6H), 7.76(d, J=8.8 Hz, 6H), 7.65(d, J=8.8 Hz, 6H), 7.41(s, 24H), 7.31-7.25(m, 12H), 7.02(d, J=8.0 Hz, 6H), 6.73(d, J=8.0 Hz, 6H). ^{13}C NMR (100 MHz, $CDCl_3$, TMS standard, 30 °C, ppm): δ 170.23, 152.71, 141.59, 140.13, 139.78, 137.43, 137.43, 135.64, 131.00, 130.69, 128.21, 126.65, 126.35, 125.85, 125.44, 124.23,123.10, 120.27, 119.78, 119.69, 111.23, 109.59. MALDI-TOF-MS: 2024.3 ($[M + H]^+$ calcd for $C_{147}H_{90}N_{12}$: 2022.7).

G3 Dendrimer. The previous procedure was followed using 0.494 g (0.365 mmol) of the G3 monomer, 0.123 g (1.09 mmol) of DABCO, and 0.052 g (0.274 mmol) of $TiCl_4$ in chlorobenzene (5.5 mL), to produce the G3 dendrimer as a yellow powder in 95% yield (0.459 g). ^1H NMR (400 MHz, $CDCl_3$, TMS standard, 30 °C, ppm): δ 8.52(m, 168H), 6.75(m, 6H). ^{13}C NMR (100 MHz, $CDCl_3$, TMS standard, 30 °C, ppm): δ 170.15, 152.72, 141.64, 141.40, 140.63, 140.35, 139.47, 137.74, 135.60, 131.16, 130.18, 130.01, 129.46, 128.13, 126.46, 126.22, 125.78, 125.43, 124.34, 123.69, 123.60, 123.01, 120.21, 119.60, 111.71, 111.13, 109.57. MALDI-TOF-MS: 4009.6 ($[M + H]^+$ calcd for $C_{291}H_{174}N_{24}$: 4003.4).

Acknowledgement

This work was partially supported by CREST from Japan Science and Technology Agency, Grants-in-Aid for Scientific Research (Nos. 15036262, 15655019、15350073) and the 21st COE Program (Keio-LCC) from the Ministry of Education, Science, Culture and Sports, and a Research Grant(Project No. 23) from Kanagawa Academy Science and Technology.

[1] F. E. Goodson, S. I. Hauck, J. F. Hartwig, *J. Am. Chem. Soc.* **1999**, *121*, 7527.

[2] T. D. Selby, S. C. Blackstock, *Org. Lett.* **1999**, *1*, 2053.

[3] [3a] J. Louie, J. F. Hartwig, *J. Am. Chem. Soc.* **1997**, 119, 11695; [3b] T. D. Selby, S. C. Blackstock, *J. Am. Chem. Soc.* **1998**, *120*, 12155; [3c] M. I. Ranasinghe, O. P. Varnavski, J. Pawlas, S. I. Hauck, J. Louie, J. F. Hartwig, T. Goodson III, *J. Am. Chem. Soc.* **2002**, *124*, 6520.

[4] C. W. Tang, S. A. VanSlyke, *Appl. Phys. Lett.* **1987**, *51*, 913.

[5] U. Bach, D. Lupo, P. Conte, J. E. Moser, F. Weissörtel, J. Salbeck, H. Spreitzer, M. Grätzel, *Nature,* **1998**, *395*, 583.

[6] M. Higuchi, S. Shiki, K. Ariga, K. Yamamoto, *J. Am. Chem. Soc.* **2001**, *123*, 4414.

[7] [7a] J. Hofkens, M. Maus, T. Gensch, T. Vosch, M. Cotlet, F. Köhn, A. Herrmann, K. Müllen, F. De Schryver, *J. Am. Chem. Soc.* **2000**, *122*, 9278; [7b] M. Schlupp, T. Weil, A. J. Berresheim, U. M. Wiesler, J. Bargon, K. Müllen, *Angew Chem. Int. Ed.,* **2001**, *40*, 4011.

[8] [8a] Y. Shirota, Y. Kuwabara, H. Inada, T. Wakimoto, H. Nakada, Y. Yonemoto, S. Kawami, K. Imai, *Appl. Phys. Lett.* **1994**, *65*, 807; [8b] P.-W. Wang, Y.-J. Lin, C. Devadoss, P. Bharathi, J. S. Moore, *Adv. Mater.* **1996**, *8*, 237; [8c] A. W. Freeman, S. C. Koene, P. R. L. Malenfant, M. E. Thompson, J. M. J. Fréchet, *J. Am. Chem. Soc.* **2000**, *122*, 12385; [8d] S. C. Lo, N. A. H. Male, J. P. J. Markham, S. W. Magennis, P. L. Burn, O. V. Salata, I. D. W. Samuel, *Adv. Mater.* **2002**, *14*, 975; [8e] P. Furuta, J. Brooks, M. E. Thompson, J. M. J. Fréchet, *J. Am. Chem. Soc.* **2003**, *125*, 13165.

[9] S. A. VanSlyke, C. H. Chen, C. W. Tang, *Appl. Phys. Lett.* **1996**, *69*, 2160.

[10] [10a] F. Huang, A. G. MacDiamid, B. R. Hsieh, *Appl. Phys. Lett.* **1995**, 67, 1659; [10b] X. Zhou, M. Pfeiffer, J. Blochwitz, A. Werner, A. Nollau, T. Fritz, K. Leo, *Appl. Phys. Lett.* **2001**, *78*, 410.

[11] R. H. Partridge, *Polymer* **1997**, *81*, 3294.

[12] [12a] S. Hayashi, H. Etoh, S. Saito, *Jpn. J. Appl. Phys., Part 2* **1986**, *25*, L773; [12b] D. B. Romero, M. Schaer, L. Zuppiroli, B. Cesar, B. Francois, *Appl. Phys. Lett.* **1995**, *67*, 1659; [12c] S. A. Carter, M. Angelopoulos, S. Karg, P. J. Brock, J. C. Scott, *Appl. Phys. Lett.* **1997**, *70*, 2067; [12d] M. Gross, D. C. Müller, H-G. Nothofer, U. Scherf, D. Neher, C. Bräuchle, K. Meerholz, *Nature* **2000**, *405*, 661.

[13] [13a] Y. Yang, A. J. Heeger, *Appl. Phys. Lett.* **1994**, *64*, 1245; [13b] J. R. Sheets, H. Antoniadis, M. R. Hueschen, W. Lepnard, J. Miller, R. Moon, D. Roitman, A. Stocking, *Science* **1996**, *273*, 884.

[14] Carbazole dendrimers with a conjugated backbone have been the subject of recent studies.[15]

[15] [15a] Z. Zhu, J. S. Moore, *J. Org. Chem.* **2000**, *65*, 116; [15b] N. D. McClenaghan, R. Passalacqua, F. Loiseau, S. Campagna, B. Verheyde, A. Hameurlaine, W. Dehaen, *J. Am. Chem. Soc.* **2003**, *125*, 5356.

[16] A. Kimoto, J-S. Cho, M. Higuchi, K. Yamamoto, *Chem. Lett.* **2003**, *32*, 674.

[17] C. J. Hawker, J. M. J. Fréchet, *J. Am. Chem. Soc.* **1990**, *112*, 7638.

[18] M. Higuchi, H. Kanazawa, M. Tsuruta, K. Yamamoto, *Macromolecules* **2001**, *34*, 8847.

[19] M. Higuchi, A. Kimoto, S. Shiki, K. Yamamoto, *J. Org. Chem.* **2000**, *65*, 5680.

[20] [20a] K. Yamamoto, M. Higuchi, S. Shiki, M. Tsuruta, H. Chiba, *Nature* **2002**, 415, 509; [20b] T. Imaoka, H. Horiguchi, K. Yamamoto, *J. Am. Chem. Soc.* **2003**, *125*, 340; [20c] N. Sato, J-S. Cho, M. Higuchi, K. Yamamoto, *J. Am. Chem. Soc.* **2003**, 125, 8104; [20d] M. Higuchi, M. Tsuruta, H. Chiba, S. Shiki, K. Yamamoto, *J. Am. Chem. Soc.* **2003**, *125*, 9988.

[21] The absorption band around 600 nm attributed to the complexation of $SnCl_2$ with carbazole unit has not been observed during the complexation with imine units because of the larger equilibrium constants of the imine units.

[22] [22a] M. Pfeiffer, A. Beyer, T. Fritz, K. Leo, *Appl. Phys. Lett.* **1998**, *73*, 3202; [22b] X. Zhou, J. Blochwitz, M. Pfeiffer, A. Nollau, T. Fritz, K. Leo, *Adv. Funct. Mater.* **2001**, *11*, 310; [22c] A. Yamamori, C. Adachi, T. Koyama, Y. Taniguchi, *J. Appl. Phys.* **1999**, *86*, 4369.69.

[23] [23a] A. Kimoto, J-S. Cho, K. Yamamoto, *J. Photopolym. Sci. Technol.* **2003**, *16*, 293; [23b] J-S. Cho, A. Kimoto, T. Nishiumi, K. Yamamoto, *J. Photopolym. Sci. Technol.* **2003**, *16*, 295.